Rif1 Binding and Control of Chromosome-Internal DNA Replication Origins Is Limited by Telomere Sequestration

Hafner, Lukas ; Lezaja, Aleksandra ; Zhang, Xu ; Lemmens, Laure ; Shyian, Maksym ; Albert, Benjamin ; Follonier, Cindy ; Nunes, Jose Manuel ; Lopes, Massimo ; Shore, David ; Mattarocci, Stefano

Abstract: The Saccharomyces cerevisiae telomere-binding protein Rif1 plays an evolutionarily conserved role in control of DNA replication timing by promoting PP1-dependent dephosphorylation of replication initiation factors. However, ScRif1 binding outside of telomeres has never been detected, and it has thus been unclear whether Rif1 acts directly on the replication origins that it controls. Here, we show that, in unperturbed yeast cells, Rif1 primarily regulates late-replicating origins within 100 kb of a telomere. Using the chromatin endogenous cleavage ChEC-seq technique, we robustly detect Rif1 at late-replicating origins that we show are targets of its inhibitory action. Interestingly, abrogation of Rif1 telomere association by mutation of its Rap1-binding module increases Rif1 binding and origin inhibition elsewhere in the genome. Our results indicate that Rif1 inhibits replication initiation by interacting directly with origins and suggest that Rap1-dependent sequestration of Rif1 increases its effective concentration near telomeres, while limiting its action at chromosome-internal sites.

DOI: https://doi.org/10.1016/j.celrep.2018.03.113

Report

Cell Reports

Rif1 Binding and Control of Chromosome-Internal DNA Replication Origins Is Limited by Telomere Sequestration

Graphical Abstract

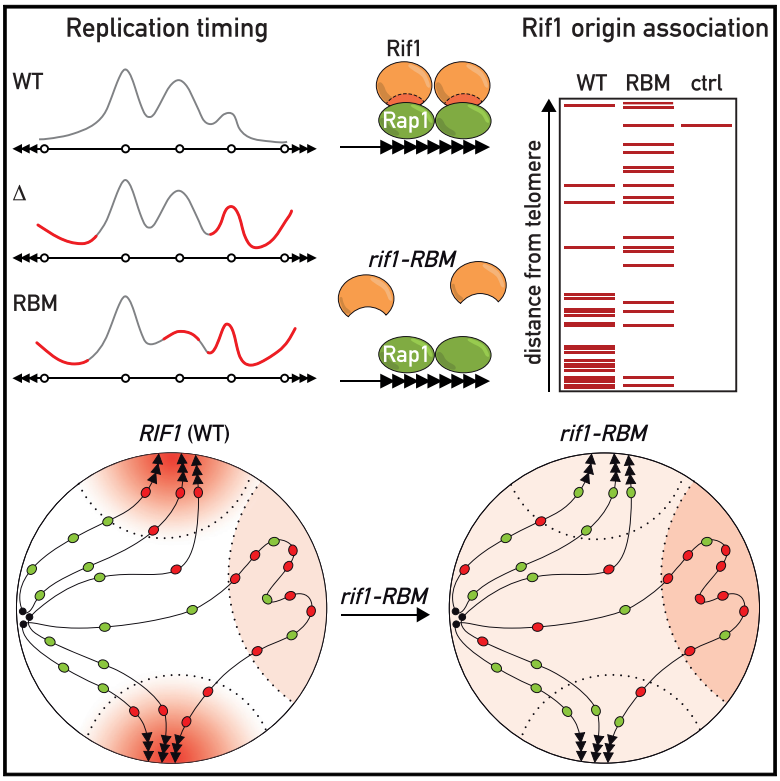

Authors

Lukas Hafner, Aleksandra Lezaja, Xu Zhang, ..., Massimo Lopes, David Shore, Stefano Mattarocci

Correspondence

david.shore@unige.ch (D.S.), stefano.mattarocci@unige.ch (S.M.)

In Brief

Hafner et al. use cell-sorting assays and chromatin endogenous cleavage sequencing (ChEC-seq) to characterize the repressive effect of Rif1 protein on DNA replication initiation. They find that global replication dynamics are controlled by telomeric sequestration of Rif1 by the telomere repeat binding protein Rap1.

Highlights

- Rif1 binds directly to DNA replication origins that it regulates
- Sequestration through Rap1 binding promotes Rif1 targeting to telomere-proximal origins
- Genome-wide replication dynamics are altered by cell synchronization

Data and Software Availability

GSE97953

Hafner et al., 2018, Cell Reports *23*, 983–992
April 24, 2018
https://doi.org/10.1016/j.celrep.2018.03.113

CellPress

Cell Reports
Report

Rif1 Binding and Control of Chromosome-Internal DNA Replication Origins Is Limited by Telomere Sequestration

Lukas Hafner,[1,2,6] Aleksandra Lezaja,[1,2,5,7] Xu Zhang,[1,2,5] Laure Lemmens,[1,2,5] Maksym Shyian,[1,2] Benjamin Albert,[1,2] Cindy Follonier,[3,8] Jose Manuel Nunes,[2,4] Massimo Lopes,[3] David Shore,[1,2,*] and Stefano Mattarocci[1,2,9,*]
[1]Department of Molecular Biology, University of Geneva, Geneva, Switzerland
[2]Institute of Genetics and Genomics of Geneva (iGE3), Geneva, Switzerland
[3]Institute of Molecular Cancer Research, University of Zurich, Zurich 8057, Switzerland
[4]Department of Genetics and Evolution, University of Geneva, Geneva, Switzerland
[5]These authors contributed equally
[6]Present address: Institut Pasteur, Biology of Infection Unit, Paris, France
[7]Present address: Department of Molecular Mechanisms of Disease, University of Zurich, Zurich, Switzerland
[8]Present address: Department of Molecular Biology, Princeton University, Princeton, NJ 08540, USA
[9]Lead Contact
*Correspondence: david.shore@unige.ch (D.S.), stefano.mattarocci@unige.ch (S.M.)
https://doi.org/10.1016/j.celrep.2018.03.113

SUMMARY

The *Saccharomyces cerevisiae* telomere-binding protein Rif1 plays an evolutionarily conserved role in control of DNA replication timing by promoting PP1-dependent dephosphorylation of replication initiation factors. However, ScRif1 binding outside of telomeres has never been detected, and it has thus been unclear whether Rif1 acts directly on the replication origins that it controls. Here, we show that, in unperturbed yeast cells, Rif1 primarily regulates late-replicating origins within 100 kb of a telomere. Using the chromatin endogenous cleavage ChEC-seq technique, we robustly detect Rif1 at late-replicating origins that we show are targets of its inhibitory action. Interestingly, abrogation of Rif1 telomere association by mutation of its Rap1-binding module increases Rif1 binding and origin inhibition elsewhere in the genome. Our results indicate that Rif1 inhibits replication initiation by interacting directly with origins and suggest that Rap1-dependent sequestration of Rif1 increases its effective concentration near telomeres, while limiting its action at chromosome-internal sites.

INTRODUCTION

DNA replication initiation in budding yeast occurs at precise genomic loci called replication origins, defined by an 11-bp autonomous replicating sequence (ARS) consensus sequence (ACS). The activity of two kinases, cyclin-dependent kinase (CDK) and Dbf4-dependent kinase (DKK), is required for the initiation of DNA replication, a tightly regulated process referred to as origin firing (Siddiqui et al., 2013).

Interestingly, not all potential origins fire during each cell cycle, nor do active origins all fire at the same time. This characteristic temporal pattern of origin firing is established in G1 phase, but the mechanisms underlying this process are still poorly understood (Rhind and Gilbert, 2013). According to a current model, the efficiency and timing of origin firing is determined by the availability of a set of limiting factors, as well as the capacity of individual origins to recruit these factors (Mantiero et al., 2011).

The budding yeast Rif1 protein (ScRif1), involved in telomere length homeostasis through its interaction with the TG_{1-3} repeat binding protein Rap1 (Mattarocci et al., 2016), has recently been shown to affect DNA replication timing at many sites throughout the genome (Peace et al., 2014). ScRif1 inhibits origin firing by counteracting DDK activity through its interaction with the Glc7/PP1 phosphatase (Davé et al., 2014; Hiraga et al., 2014; Mattarocci et al., 2014; Sreesankar et al., 2012). However, it is unclear whether ScRif1 acts directly at replication origins since its binding has so far only been detected at telomeres and silent mating-type loci (Park et al., 2011). In fission yeast *S. pombe*, Rif1 has been shown to bind to G quadruplex structures and to influence origin firing over relatively long distances (up to 50 kb) (Hayano et al., 2012; Kanoh et al., 2015). Significantly, the role of Rif1 in DNA replication timing is conserved from yeast to mammals (Mattarocci et al., 2016).

In this study, we first tried to elucidate precisely which origins Rif1 regulates, using several different methods to measure DNA replication dynamics. We then applied the chromatin endogenous cleavage (ChEC) method (Schmid et al., 2004) coupled to deep sequencing (ChEC-seq; Zentner et al., 2015) to identify sites of Rif1 binding genome-wide. This allowed us to detect Rif1 association at origins, mostly telomere-proximal and displaying Rif1-modulated firing. Finally, we show that Rif1 is sequestered at telomeres through its interaction with the protein Rap1 and that this limits its binding and function at chromosome-internal origins.

RESULTS AND DISCUSSION

ScRif1 Affects the Timing of DNA Polε Recruitment to Replication Origins in Cells Released from a G1 Block

To quantify the effect of Rif1 on replication timing, we first used chromatin immunoprecipitation (ChIP) of DNA polymerase

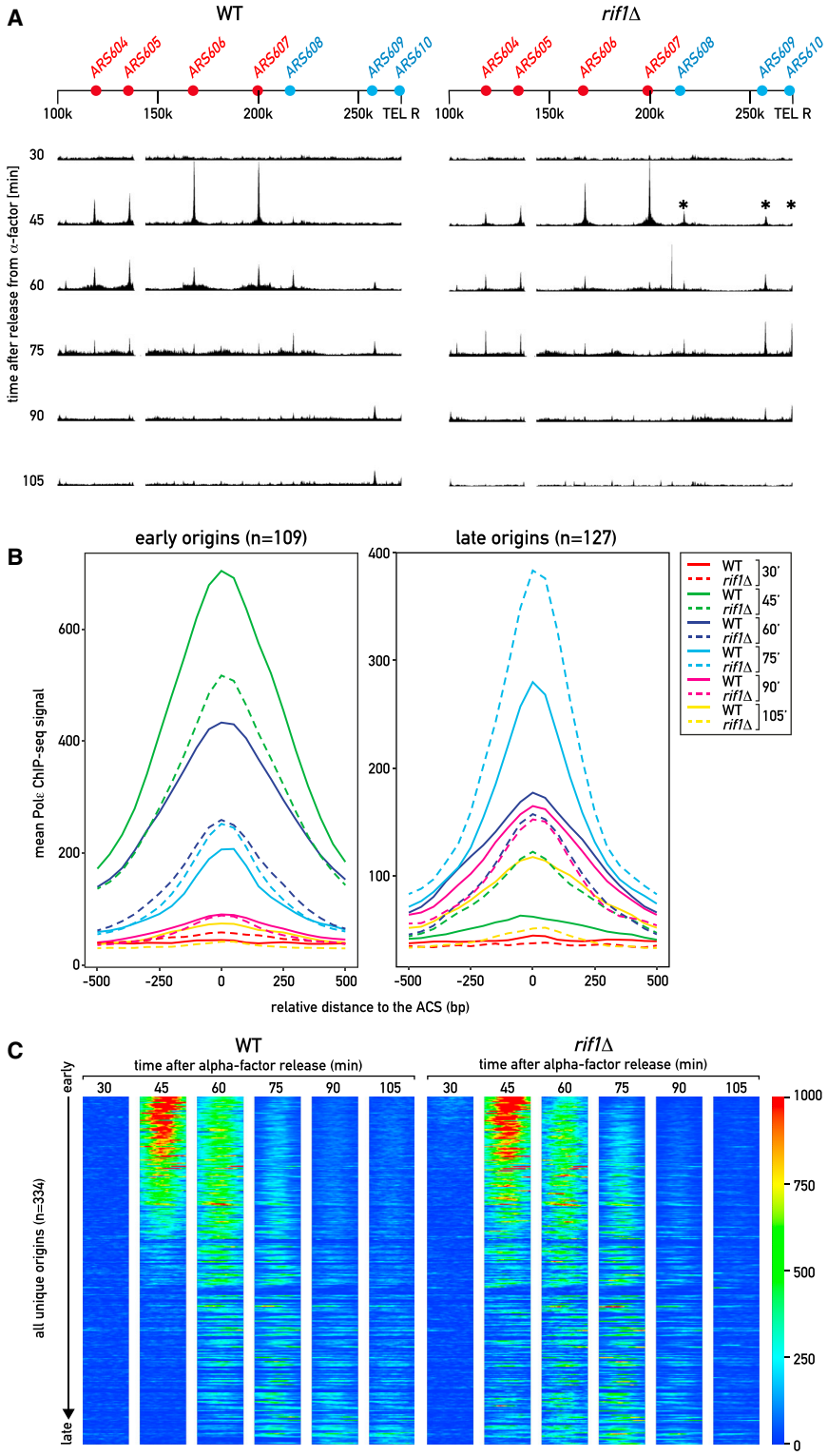

Figure 1. Deletion of *RIF1* Affects the Recruitment of Polε to Replication Origins

(A) Polε-Myc ChIP-seq signals at chromosome VI (100–270 kb) at the indicated times following release at 18°C from an α-factor block. Early and late origins are indicated in red and blue, respectively. *Late origins affected by deletion of *RIF1*.

(B) Average plots showing Polε recruitment at early- and late-origin sets (Soriano et al., 2014) at the indicated time points following release from an α-factor block at 18°C. Y axis represents the mean ChIP-seq signal (read counts) for the indicated origin classes. Continuous and dashed lines show, respectively, data for WT and *rif1Δ* cells.

(C) Heatmap of Polε-Myc ChIP-seq signals measured at regions surrounding 334 unique origins present in the yeast genome (± 250 bp, centered on the ACS; Table S1). The origins are ordered according to replication timing as measured in the WT strain.

See also Figures S1 and S2 and Tables S1 and S2.

epsilon (Polε) in cells released into S phase from an α-factor induced G1 arrest (Bianchi and Shore, 2007). To determine the genome-wide effect of Rif1 on Polε recruitment and movement, we compared wild-type (WT) and *rif1Δ* cells by Polε ChIP-seq at different time points after release (see Figure S1A for fluorescence-activated cell sorting [FACS] analysis). Clear peaks appeared at origins in WT cells when they were expected to fire (Figure 1A, left panel; e.g., early ARSs *604–607* at 45 min; late ARSs *608–610* at 60–75 min). Interestingly, these initial peaks diminished but did not disappear over multiple time points (Figures 1A and 1C), perhaps reflecting a lag between recruitment and origin firing or a failure of some origins with Polε loaded to fire. We found that *rif1Δ* caused significantly earlier recruitment at all three of these late-replicating telomere-proximal sites (Figure 1A, right panel) and obtained similar results for origins close to the end of chromosome I-L (Figure S1B). This effect is not due to telomere elongation caused by chronic absence of Rif1 (as in *rif1Δ* cells), because we observed the same phenotype after only 1 hr of anchor-away depletion of Rif1 (Haruki et al., 2008; Shyian et al., 2016), during which time telomere elongation is negligible (Figure S1C).

Examining the 334 unique *S. cerevisiae* origins (Siow et al., 2012; Table S1), we found that Polε is recruited on average to late origins earlier in *rif1Δ* than in WT cells (Figure 1B, right panel). Interestingly, early origins tended to recruit less Polε in the absence of Rif1 (Figure 1B, left panel), which might be due to redistribution of limiting factors (Mantiero et al., 2011; Peace et al., 2014). When we sorted the 334 origins by their firing time in WT cells, many mid- and late-firing origins showed enrichment

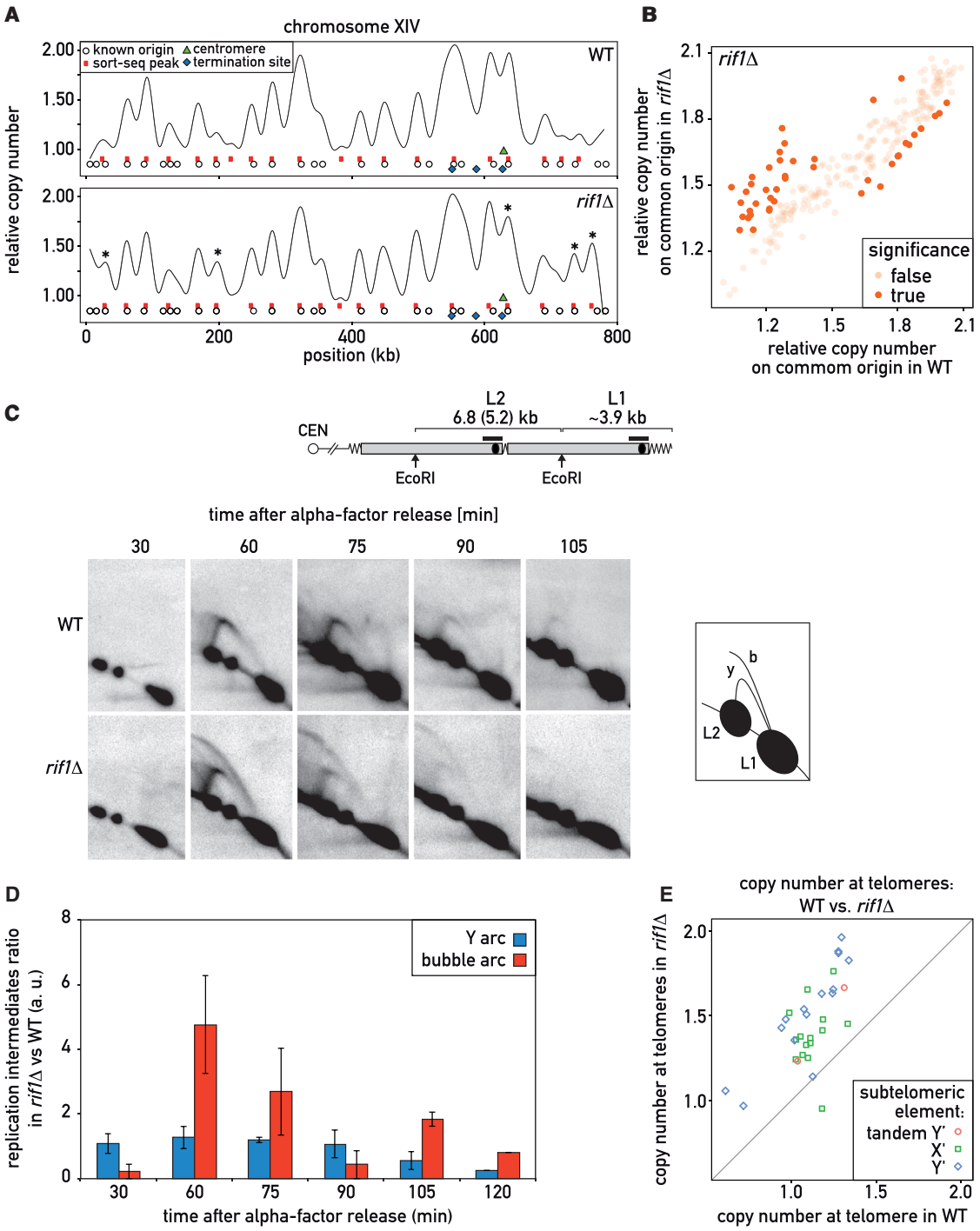

Figure 2. Replication Dynamics in Unperturbed Cells Measured by Sort-Seq

(A) Comparison of the replication profiles of chromosome XIV in unperturbed WT (top panel) and *rif1Δ* (bottom panel) cells. *Origins where we observed a significant difference between the two strains (see Experimental Procedures and Figure S2B for details).

(B) Plot comparing relative copy number, as measured by sort-seq, of active origins in *rif1Δ* (y axis) versus WT (x axis) cells. Significant differences ($p < 0.05$) are represented as dark-colored dots.

(C) 2D-gel electrophoresis of EcoRI-digested genomic DNA from WT and *rif1Δ* cells, prepared at the indicated times following release from an α-factor block, blotted and probed for sub-telomeric Y′ sequences. The schematic (above) depicts the structure of a telomere containing tandem Y′ elements, with black circles indicating origin locations and black bars the probe sequence. The diagram on the right indicates the location of the linear L1 and L2 fragments as well as the "Y" and "bubble" (b) arcs resulting from replication intermediates.

(legend continued on next page)

in Polε signal at earlier time points in *rif1Δ* compared to WT cells (e.g., 45 and 60 min; Figure 1C). We found that *rif1Δ* leads to earlier Polε recruitment at 115 origins and a delay of Polε recruitment at 49 origins, while 170 origins were unaffected (Figure S1D; Table S1; Supplemental Experimental Procedures). Notably, late origins tend to cluster near telomeres (Figure S1E; Soriano et al., 2014).

The classes defined in Table S1 overlap well with those described in a previous study (Peace et al., 2014): > 75% of Rif1-affected origins were in the corresponding class (activated/repressed) in this study (Table S2, top; see Figure S1F for details). In summary, we show that DNA Polε recruitment is accelerated at late-firing origins throughout the genome in *rif1Δ* cells released from an α-factor block, consistent with previous findings that used bromodeoxyuridine (BrdU) incorporation or density shift measures of replication initiation (Lian et al., 2011; Peace et al., 2014).

Deletion of RIF1 Causes Early Replication of Origins Proximal to Telomeres in Unperturbed Cells

Until now, all DNA replication timing experiments in *rif1Δ* strains have been performed in cells released from either a physiological (α factor pheromone) (Figure 1) or a genetic (*cdc7*) cell-cycle block (Davé et al., 2014; Hiraga et al., 2014; Lian et al., 2011; Mattarocci et al., 2014; Peace et al., 2014; Shyian et al., 2016). Such blocks might affect the replication initiation regulatory machinery, which is coupled to the cell cycle. We thus decided to measure DNA replication in a way that avoids cell-cycle arrest, using the sort-seq method (Müller et al., 2014), which quantifies DNA copy number by deep sequencing of unperturbed FACS-sorted S-phase cells (Figure S2A).

Using sort-seq, we found that both WT and *rif1Δ* cells employ a very similar subset of origins (Table S3; Figures 2A and S2B). The vast majority of origins/origin clusters (202/247) showed no difference between WT and *rif1Δ*, whereas 33 clusters (comprising 53 distinct confirmed or likely origins) showed a higher and 12 a lower relative copy number in *rif1Δ* compared to WT (Table S3). Most origins with a higher copy number in *rif1Δ* were late origins. By contrast, those origin/origin clusters with decreased copy number in *rif1Δ* tended to be early or mid-S phase firing in WT cells (relative copy number from 1.45 to 2.0; Figure 2B). These results differ from those obtained in synchronized cells, where *rif1Δ* was found to increase BrdU incorporation at 174 origins, with 81 origins showing lower signals (Peace et al., 2014) (see above for Polε association).

We also performed a 2D gel analysis of DNA replication intermediates at sub-telomeric Y′ elements in cells released from a G1 block (Figure 2C). As observed previously (Makovets et al., 2004), Y′ elements are primarily replicated from an adjacent origin, as demonstrated by the presence of a strong "Y-arc" signal and rarely replicated from their endogenous origin (weak "bubble arc" signal). However, in *rif1Δ* cells we observed a strong increase in bubble arc intensity, indicating a higher efficiency of origin firing at these sub-telomeric loci (Figures 2C and 2D). In support of this conclusion, sort-seq revealed a copy number increase immediately adjacent to 30 of 32 telomeres (including nearly all identifiable Y′ junctions) in *rif1Δ* cells, compared to WT (Figure 2E), as well as earlier Polε arrival at Y′ sequences (Figure S2C). This suggests that Y′ origins (and sub-telomeric origins in general) are regulated by Rif1 in synchronized and unperturbed cells.

In summary, our findings indicate that Rif1 regulates telomere-proximal origin firing in unperturbed, exponentially growing cells, but reveal a much subtler effect than that obtained by measuring BrdU incorporation or Polε recruitment in G1-blocked cells released into a synchronous S phase.

Rif1-MNase ChEC-Seq Reveals Rif1 Binding at Telomere-Proximal Replication Origins

Rif1 binds the distal TG_{1-3} repeats at telomeres and the silent *HM* loci through its interaction with Rap1 (Shi et al., 2013), suggesting that it could directly regulate replication timing at the *ARS* elements found at these specific sites. But how does Rif1 control other origins far from these sites? Since we failed to detect Rif1 at other loci by ChIP-seq (unpublished data), we decided to explore Rif1 binding using the ChEC method (Schmid et al., 2004), adapted for genome-wide analysis (ChEC-seq; Zentner et al., 2015). To perform a ChEC analysis, we fused the MNase gene to the C terminus of the chromosomal copy of *RIF1* and used a strain carrying MNase driven by the strong *REB1* promoter as a control ("free MNase"). Rif1-MNase showed a slight rescue of the *cdc7-4 ts* phenotype (see Figure S3A), though less than other *RIF1* mutants (Mattarocci et al., 2014; see below), probably due to lower protein levels (Figure S3B). Nevertheless, since the Rif1-MNase strain showed much more rapid telomere degradation compared to free MNase in a ChEC assay probed by Southern blot (Figure S3C), we carried out a ChEC-seq analysis. This revealed specific binding of Rif1 to many replication origins that it regulates. For example, we found a significant ChEC-seq signal at the late-origin *ARS609*, but not at the nearby early-origin *ARS607* (Figure 3A; see Figure S3D for other examples). At telomeres, as expected, the Rif1-MNase signal was particularly high compared to free MNase (Figures 3A and S3D).

To obtain a more quantitative picture of Rif1-MNase chromatin binding genome-wide, we performed a time-course ChEC-seq experiment by taking samples at different time points after MNase activation. Focusing first on all confirmed and likely origins sorted by their distance from a telomere, we found that Rif1-MNase cleavage is strongly enriched at origin sites (± 250 bp from ACS) within ~50–100 kb of telomeres, compared to more telomere-distal origins (Figure 3B; see Supplemental Experiment Procedures for details). These telomere-proximal origins displayed a rapid and strong increase in Rif1-MNase signal,

(D) Quantification of three independent 2D-gel electrophoresis experiments (as in C). Red bars: ratio of the bubble arc intensity in *rif1Δ* compared to WT. Blue bars; y arc intensity in *rif1Δ* compared to WT. Error bars indicate SD.

(E) Comparison of relative copy number, as measured by sort-seq, for all distinguishable sub-telomeric features (as indicated), in WT (x axis) versus *rif1Δ* (y axis) cells.

See also Figure S2 and Table S2.

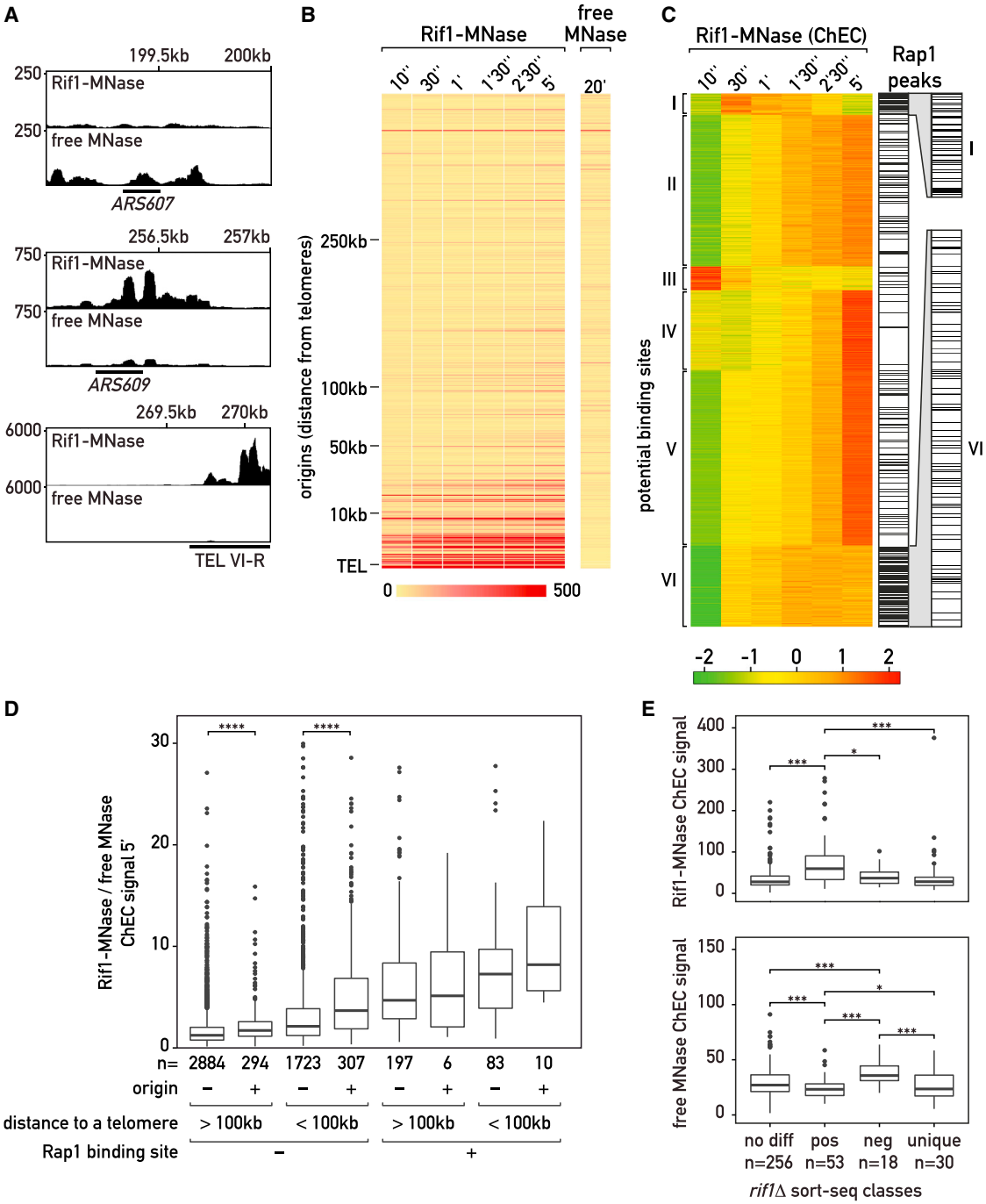

Figure 3. Detection of Rif1 Binding Sites Genome Wide

(A) Genome browser screen shots of ChEC-seq signal (normalized read counts; y axis) from Rif1-MNase- and free MNase-expressing cells at the indicated loci on chromosome VI-R (x axis; *ARS607*, early ARS; *ARS609*, late ARS). The Rif1-MNase data are from a sample taken at 2 min 30 s following Ca^{2+} addition, whereas the free MNase data are from a 20-min time point.

(B) ChEC-seq mean signal at likely and confirmed origins (±250 bp) (Siow et al., 2012) for the indicated times following Ca^{2+} addition in a strain expressing Rif1-MNase. Origins are sorted according to their distance from a telomere. Data for a strain expressing free MNase (20 min following Ca^{2+} addition) are shown to the right, accompanied by a key indicating the magnitude of the mean ChEC signal.

(C) Heatmap of 5,504 peaks (rows) of Rif1-MNase signal enrichment. Sites were clustered according to *Z* scores (color scale) for the indicated time course following Ca^{2+} addition (see Table S4). *Z* scores were calculated over each row and indicate the evolution of the signal over time (Zentner et al., 2015). Sites where a peak of Rap1 binding (Knight et al., 2014) overlaps with the ChEC-seq peak are indicated to the right, with clusters I and VI expanded (far right).

(legend continued on next page)

but little or no enrichment even after 20 min of free MNase exposure (Figure 3B).

We next calculated a *Z* score for the ChEC-seq signals at all time points (Zentner et al., 2015) and clustered peaks displaying similar cleavage dynamics (Figure 3C). This revealed 6 distinct clusters, including not only the many novel origin-associated peaks of Rif1-MNase cleavage, but a large number (~5,500) of additional peaks representing potential Rif1 binding sites (Figure 3C; see Supplemental Experimental Procedures for details). We note that peaks are often clustered together (Figures 3A and S3D) and probably representative of single binding events, as noted recently for ChEC-seq of yeast transcription factors (Zentner et al., 2015). Interestingly, given the known direct physical interaction of Rif1 with the Rap1 protein (Shi et al., 2013), we found that two of the six classes (I and VI) were strongly enriched for the Rap1 motif and overlap with a peak of Rap1 binding detected by ChIP-seq (Knight et al., 2014; Figures 3C and S3E). Many of these are promoter-associated Rap1 peaks, perhaps reflecting transient interactions where only one or two Rap1 molecules are present. Importantly, many, if not all of the Rif1-MNase peaks associated with replication origins (or a Rap1 binding site) are likely to result from specific binding of Rif1 *in vivo*, since they display a higher average enrichment compared to peaks not associated with either feature (Figure 3D). Nevertheless, a small number of Rif1 peaks unlinked to either origins or Rap1 sites appear to be quite strong. Further study will be required to determine whether these peaks are connected in some way to Rif1 function.

Rif1-Repressed Origins Identified by Sort-Seq Are Bound by Rif1

To determine whether the origins affected by *rif1Δ* in unperturbed cells (Table S3) indeed correspond to those bound directly by Rif1, we compared our sort-seq and ChEC-seq datasets (Figure 3E, upper panel). Significantly, Rif1-repressed origins (referred to as "pos" in the graph, see also Table S3) showed a stronger ChEC-seq signal than origins where no difference (p = 2.23e-4) or a decrease in relative copy number was detected (p = 2.78e-3) (referred as "no diff" and "neg", respectively; Table S3), or at origins where firing was detected only in *rif1Δ* (p = 8.85e-2) (referred as "unique"). No positive correlation between free MNase signal and origins repressed by Rif1 in sort-seq was found (Figure 3E, bottom panel). These findings support the hypothesis that Rif1 regulates replication directly at target origins. Interestingly, origins that were less active in *rif1Δ* (referred to as "neg" in the graphs) are enriched in free MNase signal compared to all other groups (Figure 3E, bottom panel). These are mainly early firing origins that might contain highly accessible chromatin prone to free MNase cleavage. Taken together, these data strongly suggest that Rif1 directly binds to the replication origins whose firing it regulates.

We also compared the enrichment of ChEC-seq signal at origins with our Polε-Myc ChIP-seq results (Figure 1C; Table S1) and with data for BrdU incorporation following release of G1-blocked cells (Peace et al., 2014). Both these measures of altered origin firing correlated less well with the Rif1-MNase ChEC-seq signals than did the sort-seq measurements (cf. Figures 3E and S3F). Furthermore, in a direct comparison of the effects at a common set of origins that were detected as active by sort-seq (n = 227), the positive changes measured by sort-seq (earlier firing in the absence of Rif1) correlate significantly better with the Rif1-MNase signals than do the changes measured in synchronized cells by Polε-Myc ChIP seq (Figure S3G).

Since our ChEC-seq and sort-seq results highly correlate (Figure 3E), we suggest that the differences between results from BrdU incorporation in synchronized cells (Peace et al., 2014) and unperturbed cells (Table S3) are due to an interference with the replication regulatory machinery caused by cell synchronization, and not to a lack of sensitivity of the sort-seq assay. Replication-timing decisions are taken in G1 phase (Rhind and Gilbert, 2013) when Rif1 appears to act (Davé et al., 2014; Hiraga et al., 2014; Mattarocci et al., 2014). It seems possible, then, that prolongation of the G1 phase by an α-factor block might perturb the replication timing network, particularly in cells mutated for one of its components (e.g. Rif1). These findings suggest that measurement of replication timing in unperturbed cells may provide a more accurate description of regulatory networks compared to those made in cells released from a G1 block.

Domains of Rif1 Differentially Affect Late-Origin Firing

Two functional motifs in ScRif1 have been characterized recently: the C-terminal RBM required for Rif1 recruitment to Rap1 arrays at telomeric TG_{1-3} repeats (Shi et al., 2013) and the N-terminal RVxF/SILK motif responsible for Rif1's interaction with the PP1 phosphatase (Davé et al., 2014; Hiraga et al., 2014; Mattarocci et al., 2014; Sreesankar et al., 2012). The *rif1-RBM* mutation affects telomere length regulation (Shi et al., 2013; Figure S3H), but not Rif1's ability to counteract DDK activity (Figure S3I). Conversely, the *rif1-RVxF/SILK* allele causes only a small increase in telomere length (Figure S3H), while it significantly rescues *cdc7-4 ts* lethality (Mattarocci et al., 2014; Figure S3I).

In order to evaluate the importance of these motifs in replication timing regulation, we performed sort-seq in *rif1-RBM* and

(D) Boxplot of Rif1-MNase signals over free MNase at all 5,504 peaks shown in (C). Different boxplots show different categories of peaks according to the presence of Rap1 binding site (Knight et al., 2014), to the distance to a telomere (< or >100 Kb) and to the coincidence of an ACS (±250 bp). Two-tailed Whitney-Mann test was used for statistical significance (from left to right between similar classes with or without the presence of an ACS): p = 7.50e-14, p = 4.02e-18, p = 0.905, p = 0.503. ****p = 0.001.

(E) Boxplot of Rif1-MNase (upper) and free MNase ChEC-seq (bottom) mean signal (center ± 500 bp) for each of the four different origin classes defined by their firing behavior in *rif1Δ* compared to WT, as measured by sort-seq (see text for details). Origin classifications are given in Table S3. Statistical significance was evaluated using a two-tailed Mann-Whitney test: for upper panel (no difference/pos, p = 2.1902e-06; pos/neg, p = 0.08265; pos/unique, p = 0.007368) and for lower panel (no difference/pos, p = 0.001506; no difference/neg, p = 0.000856; pos/neg, p = 5.5742e-06; neg/unique, p = 0.004756; pos/unique, p = 0.05789). *p =0.1, **p = 0.05, ***p = 0.01.

See also Figure S3 and Table S4.

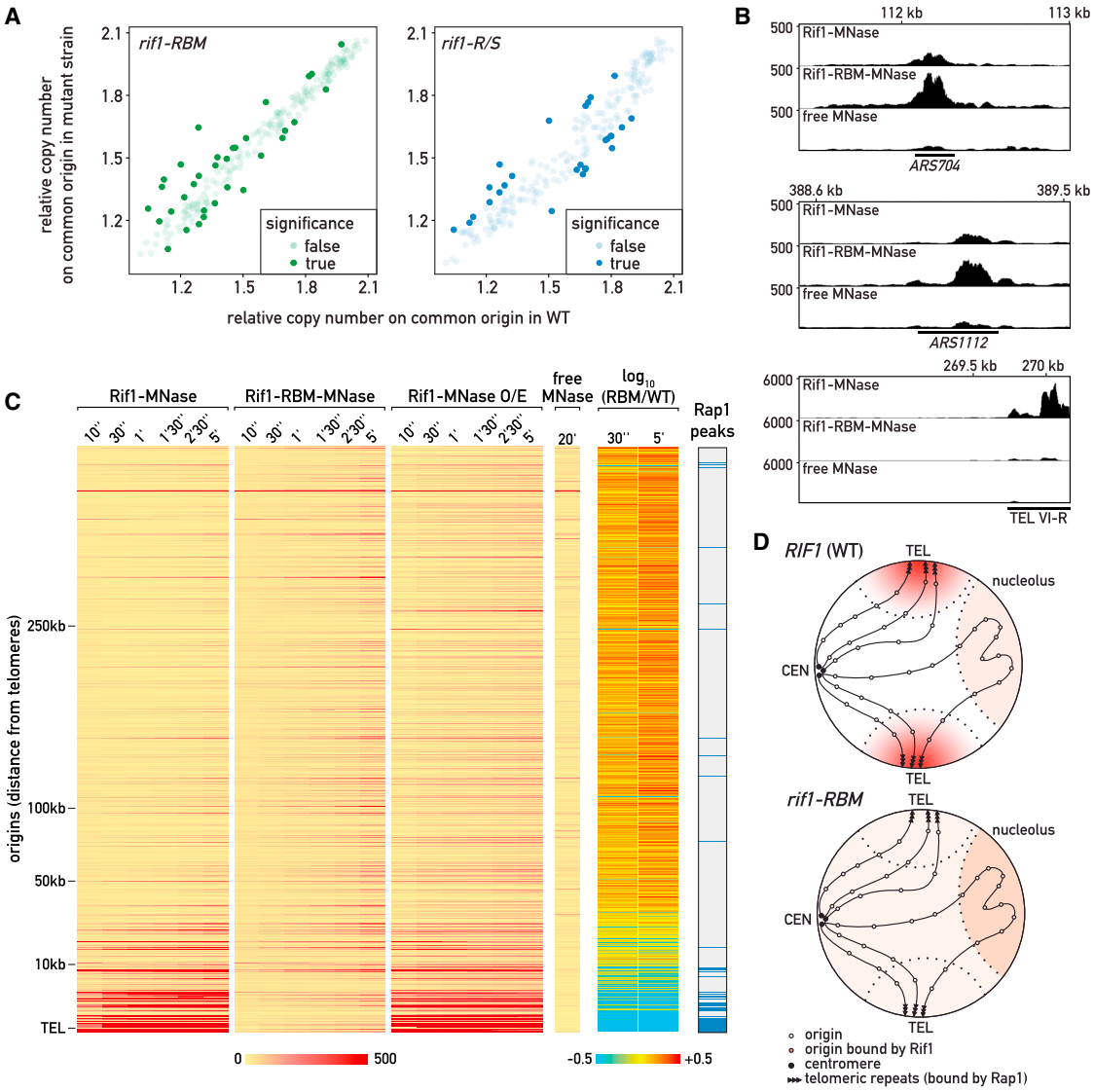

Figure 4. Role of Rif1 RBM Motif in DNA Replication Timing Control

(A) Plot comparing relative copy number, as measured by sort-seq, of active origins in *rif1-RBM* (top, green) and *rif1-RVxF/SILK* (bottom, blue) mutants versus WT cells, as in Figure 2B.

(B) ChEC-seq signals (y axis, normalized read count) from Rif1-MNase, rif1-RBM-MNase and free MNase cells at two late ARSs (*ARS704* and *ARS1112*) and at TEL VI-R (x axis). The Rif1-MNase and rif1-RBM-MNase data are from a sample taken at 2 min 30 sec following Ca^{2+} addition, whereas the free MNase data are from a 20-min time point.

(C) Heatmaps showing Rif1-MNase, rif1-RBM-MNase and overexpressed (O/E) Rif1-MNase ChEC-seq signals at all 334 likely and confirmed origins, sorted according to their distance from a telomere (Siow et al., 2012) at the indicated times following Ca^{2+} addition. Data for a free MNase sample (20 min time point) are shown to the right of these maps, followed by heatmaps of the $\log_{10}$ ratio of rif1-RBM-MNase to Rif1-MNase signals at 30 sec and 5 min. Sites where Rap1 peaks map within ± 500 bp of the ACS of the origin are indicated at the right (Rap1 peaks).

(D) (upper panel) Rif1's distribution (red) at replication origins throughout the nucleus (open circles) is sequestrated, through its binding to Rap1, to chromosomal regions in spatial proximity to telomeres and, through an unidentified mechanism, to the *rDNA* locus. (bottom panel) Upon the disruption of the Rif1-Rap1 interaction (*rif1-RBM* mutant), the gradient of Rif1 concentration is lost and Rif1 is more equally distributed throughout the whole nucleus, whereas its concentration at the *rDNA* locus is increased.

See also Figures S3 and S4 and Table S3.

rif1-RVxF/SILK mutants (Figures 4A and S4A). Neither of these two alleles causes a phenotype as drastic as *rif1Δ*, but both lead to an increase of the average relative copy number at telomeres and telomere-proximal regions (Figure S3J). The minor effect of the RVxF/SILK mutation on the global replication profile was unexpected in light of its strong suppression of *cdc7-4*. We propose that the weakened activity of Rif1-RVxF/SILK protein is still sufficient to maintain a near normal replication profile

when DDK activity is at WT levels (as in *CDC7* cells), with only a few telomere-distal origins showing a difference in their replication profile (Figure 4A).

Rif1 Origin Binding Is Regulated by Rap1-Dependent Telomere Sequestration

We noticed that some relatively inactive, late-replicating origins/origin clusters at non-telomeric sites become even less active in the *rif1-RBM* mutant, but not in *rif1-RVxF/SILK* or *rif1Δ* cells (compare origins whose relative copy number is below 1.5 in Figure 2B with those in Figure 4A). We speculated that this could be due to the release of pools of Rif1 from telomeres in *rif1-RBM* cells, which would free the protein to interact with chromosome-internal regions.

To test this hypothesis, we performed ChEC-seq in rif1-RBM-MNase cells (Figure 4B: see Figure S3B for rif1-RBM-MNase protein level measurements). Cluster analysis of rif1-RBM-MNase cleavage dynamics failed to find Rap1 binding site enrichment in any of the 6 clusters identified, as expected. We next compared the rif1-RBM-MNase signal evolution at replication origins to WT Rif1-MNase, again sorting the origins by their distance from telomeres (Figure 4C). This revealed a striking decrease of signal at sub-telomeric and telomere-proximal origins, extending over 10 kb from telomere ends, caused by disruption of the Rif1-Rap1 interaction (see Figures 4B and S4E for specific telomere examples, Figure S4B for an expanded view of telomere-proximal origins, Figures S4C and S4D for sub-telomeric elements). This result supports the hypothesis that the disruption of the Rif1-Rap1 interaction decreases the effective concentration of Rif1 across a large sub-telomeric domain. At sub-telomeric X and Y′ elements, both of which contain origins with nearby Rap1 peaks, the decrease in Rif1 binding caused by the RBM mutation is particularly strong (Figures S4C and S4D). Nevertheless, this decrease also occurred at many telomere-proximal origins without local Rap1 binding (Figure S4E). Conversely, for many origins farther from telomeres, and not Rap1-associated, the Rif1-RBM mutant showed higher ChEC signal compared to WT (Figure 4B, for examples of two telomere-distal late *ARS*s; Figure 4C, red signal in the RBM/WT heatmap). One notable example of this effect is seen at the repetitive *rDNA* locus, where Rif1 inhibits the firing of an origin present in each of the 150–200 *rDNA* copies (Shyian et al., 2016). Two sites of enhanced Rif1-MNase cleavage are detected in the *rDNA*: one at the promoter of *TAR1*, which contains a Rap1 binding site, and a second at the *rDNA* origin, where no nearby Rap1 binding is observed (Figure S4F). Strikingly, rif1-RBM-MNase cleavage is reduced to background at the *TAR1* promoter but increases compared to WT at the *rDNA* origin.

The rif1-RBM ChEC-seq result suggests that the increase of the Rif1 concentration in the nucleus caused by releasing Rif1 from telomeres leads to a proportional increase of binding at other origins. To determine whether WT Rif1 is able to bind all replication origins, independently of the RBM mutation, we strongly overexpressed Rif1-MNase (Figure S4G) and performed a ChEC-seq analysis. In contrast to rif1-RBM, and as expected, overexpression of Rif1 increased its binding at origins within 50–100 kb of a telomere (Figure 4C). Importantly, though, the signal at replication origins further away from telomeres also increased (Figure 4C), suggesting that Rif1 can interact with many origins throughout the genome. By inference we conclude that its preference for subtelomeric (X, Y′) and telomere-proximal origins is driven by its sequestration at telomere repeats by Rap1.

It is noteworthy that, even at high protein levels (Rif1-MNase O/E), sort-seq classes better correlated with the Rif1-MNase ChEC signal than did classes derived by the two methods based on cell synchronization (Polε ChIP and BrdU-seq) (Figure S4H), reinforcing our conclusion that the cell-cycle arrest associated with synchronization could alter the DNA replicating timing program.

In summary, our findings indicate that telomeric arrays of Rap1 generate a locally high concentration of Rif1 that increases its effective concentration at telomeric-proximal origins (Figure 4D, upper panel). When this telomeric pool of Rif1 is abolished by the RBM mutation the effective concentration near telomeres decreases, while it increases at non-telomeric sites (Figure 4D, bottom panel). A similar effect has been suggested to operate on Sir proteins, which also appear to be concentrated at telomeric regions through Rap1 binding (Maillet et al., 1996; Marcand et al., 1996). We suggest that Rif1 is capable of binding all origins, but that its presence in limiting amounts, combined with its sequestration at telomeres, leads to a pattern of origin association biased toward telomeric-proximal regions.

In conclusion, we demonstrate direct binding of ScRif1 to the DNA replication origins that display Rif1-mediated firing control, many of which lie within ~50–60 kb of a telomere. Our data indicate that origins recruit Rif1 through a Rap1-independent mechanism that remains uncharacterized. Although in fission yeast Rif1 binds G-quadruplex structures sometimes found in the vicinity of origins (Hayano et al., 2012; Kanoh et al., 2015), we found no such association in budding yeast, and biochemical and structural studies failed to reveal ScRif1 binding to G-quadruplex structures (Mattarocci et al., 2017). It therefore seems that Rif1's function in origin inhibition is conserved in Eukarya (Mattarocci et al., 2016), but that targeting and perhaps some effector mechanisms have diverged. It will be interesting to see whether the novel DNA binding domain recently characterized in budding ScRif1 (Mattarocci et al., 2017) is involved in directing the protein to origins.

The establishment of late replication at telomere-proximal regions may have important consequences for genome evolution. These regions often contain gene families involved in environmental adaptation whose late replication leads to a higher rate of mutagenesis, perhaps conferring a selective advantage under fluctuating conditions (Lang and Murray, 2011). One interesting consequence of Rif1 sequestration at telomeres is the possibility that telomeric TG_{1-3} tract length variation can be exploited by the cell to modulate replication timing genome-wide. Considering the large number of genetic and physiological inputs controlling telomere length in yeast (Harari et al., 2013), this may provide cells with a mechanism to regulate replication timing according to growth signals. Future studies will be required to better understand the regulation of Rif1 location genome-wide and its potential functional consequences.

EXPERIMENTAL PROCEDURES

Strain

All yeast strains used in this study are listed in Table S5.

Growth Assays and Cell Synchronization

Cell synchronization and growth assays were performed and monitored by FACS as previously described (Mattarocci et al., 2014).

Anchor-Away Technique

The anchor-away technique was performed as described (Shyian et al., 2016; see Supplemental Experimental Procedures).

Sort-Seq Assay

Sort-seq was carried out as described (Müller et al., 2014), with minor modifications (see Supplemental Experimental Procedures).

ChEC Assay

ChEC experiments were performed as described (Schmid et al., 2004; Zentner et al., 2015) with minor modifications (see Supplemental Experimental Procedures).

Neutral-Neutral 2D Gel Electrophoresis

Cells were synchronized by α-factor arrest and released as described (Mattarocci et al., 2014). Aliquots taken following release into S phase were treated with trichloroacetic acid (TCA; final concentration 6.5%) and frozen. Genomic DNA extraction and 2D agarose gel electrophoresis were performed as described (Shyian et al., 2016; see Supplemental Experimental Procedures).

Other Molecular Methods

Southern blots were performed as described in Shi et al. (2013) and qPCR ChIP and ChIP-seq as in Knight et al. (2014) and Mattarocci et al. (2014). See Supplemental Experimental Procedures for details.

DATA AND SOFTWARE AVAILABILITY

The accession number for the genomic data presented in this publication is GEO: GSE97953 (Edgar et al., 2002; https://www.ncbi.nlm.nih.gov/geo/query/acc.cgi?token=gzezawaihduhvkp&acc=GSE97953).

SUPPLEMENTAL INFORMATION

Supplemental Information includes Supplemental Experimental Procedures, four figures, and five tables and can be found with this article online at https://doi.org/10.1016/j.celrep.2018.03.113.

ACKNOWLEDGMENTS

We thank Mylene Docquier and the iGE3 genomics platform of the University of Geneva (https://ige3.genomics.unige.ch) for performing all of the deep sequencing; Ulrich Laemmli, Teemu Ardersin and Gabriel Zentner for the ChEC assay protocols; Jean-Pierre Aubry and the flow cytometry platform (CMU, University of Geneva) for assistance with FACS; Nicolas Roggli for expert assistance with graphics and artwork; Thomas Schalch for the use of his local Galaxy server; Maria Jessica Bruzzone for comments on the manuscript; Jacques Rougemont and Philippe Jacquet for assistance with HTS Station. This study was supported by grants from the Swiss National Science Foundation (31003A_149463 to D.S.) and funds provided by the Republic and Canton of Geneva (to D.S.). L.H. and A.L. were supported by an "Excellence Masters" fellowship from the University of Geneva.

AUTHOR CONTRIBUTIONS

L.H., S.M., L.L., M.L., and D.S. conceived and designed the experiments. L.H., S.M., L.L., A.L., X.Z., B.A., M.S., and C.F. performed the experiments. L.H. and J.M.N. analyzed the sort-seq data, and L.H. analyzed the ChEC-seq data. All authors contributed to analysis of other data. L.H., S.M., and D.S. wrote the manuscript.

DECLARATION OF INTERESTS

The authors declare no competing interests.

Received: May 18, 2017
Revised: January 12, 2018
Accepted: March 24, 2018
Published: April 24, 2018

REFERENCES

Bianchi, A., and Shore, D. (2007). Early replication of short telomeres in budding yeast. Cell *128*, 1051–1062.

Davé, A., Cooley, C., Garg, M., and Bianchi, A. (2014). Protein phosphatase 1 recruitment by Rif1 regulates DNA replication origin firing by counteracting DDK activity. Cell Rep. *7*, 53–61.

Edgar, R., Domrachev, M., and Lash, A.E. (2002). Gene Expression Omnibus: NCBI gene expression and hybridization array data repository. Nucleic Acids Res. *30*, 207–210.

Harari, Y., Romano, G.H., Ungar, L., and Kupiec, M. (2013). Nature vs nurture: Interplay between the genetic control of telomere length and environmental factors. Cell Cycle *12*, 3465–3470.

Haruki, H., Nishikawa, J., and Laemmli, U.K. (2008). The anchor-away technique: Rapid, conditional establishment of yeast mutant phenotypes. Mol. Cell *31*, 925–932.

Hayano, M., Kanoh, Y., Matsumoto, S., Renard-Guillet, C., Shirahige, K., and Masai, H. (2012). Rif1 is a global regulator of timing of replication origin firing in fission yeast. Genes Dev. *26*, 137–150.

Hiraga, S., Alvino, G.M., Chang, F., Lian, H.Y., Sridhar, A., Kubota, T., Brewer, B.J., Weinreich, M., Raghuraman, M.K., and Donaldson, A.D. (2014). Rif1 controls DNA replication by directing Protein Phosphatase 1 to reverse Cdc7-mediated phosphorylation of the MCM complex. Genes Dev. *28*, 372–383.

Kanoh, Y., Matsumoto, S., Fukatsu, R., Kakusho, N., Kono, N., Renard-Guillet, C., Masuda, K., Iida, K., Nagasawa, K., Shirahige, K., and Masai, H. (2015). Rif1 binds to G quadruplexes and suppresses replication over long distances. Nat. Struct. Mol. Biol. *22*, 889–897.

Knight, B., Kubik, S., Ghosh, B., Bruzzone, M.J., Geertz, M., Martin, V., Dénervaud, N., Jacquet, P., Ozkan, B., Rougemont, J., et al. (2014). Two distinct promoter architectures centered on dynamic nucleosomes control ribosomal protein gene transcription. Genes Dev. *28*, 1695–1709.

Lang, G.I., and Murray, A.W. (2011). Mutation rates across budding yeast chromosome VI are correlated with replication timing. Genome Biol. Evol. *3*, 799–811.

Lian, H.Y., Robertson, E.D., Hiraga, S., Alvino, G.M., Collingwood, D., McCune, H.J., Sridhar, A., Brewer, B.J., Raghuraman, M.K., and Donaldson, A.D. (2011). The effect of Ku on telomere replication time is mediated by telomere length but is independent of histone tail acetylation. Mol. Biol. Cell *22*, 1753–1765.

Maillet, L., Boscheron, C., Gotta, M., Marcand, S., Gilson, E., and Gasser, S.M. (1996). Evidence for silencing compartments within the yeast nucleus: A role for telomere proximity and Sir protein concentration in silencer-mediated repression. Genes Dev. *10*, 1796–1811.

Makovets, S., Herskowitz, I., and Blackburn, E.H. (2004). Anatomy and dynamics of DNA replication fork movement in yeast telomeric regions. Mol. Cell. Biol. *24*, 4019–4031.

Mantiero, D., Mackenzie, A., Donaldson, A., and Zegerman, P. (2011). Limiting replication initiation factors execute the temporal programme of origin firing in budding yeast. EMBO J. *30*, 4805–4814.

Marcand, S., Buck, S.W., Moretti, P., Gilson, E., and Shore, D. (1996). Silencing of genes at nontelomeric sites in yeast is controlled by sequestration of silencing factors at telomeres by Rap 1 protein. Genes Dev. *10*, 1297–1309.

Mattarocci, S., Shyian, M., Lemmens, L., Damay, P., Altintas, D.M., Shi, T., Bartholomew, C.R., Thomä, N.H., Hardy, C.F., and Shore, D. (2014). Rif1 controls DNA replication timing in yeast through the PP1 phosphatase Glc7. Cell Rep. *7*, 62–69.

Mattarocci, S., Hafner, L., Lezaja, A., Shyian, M., and Shore, D. (2016). Rif1: A conserved regulator of DNA replication and repair hijacked by telomeres in yeasts. Front. Genet. *7*, 45.

Mattarocci, S., Reinert, J.K., Bunker, R.D., Fontana, G.A., Shi, T., Klein, D., Cavadini, S., Faty, M., Shyian, M., Hafner, L., et al. (2017). Rif1 maintains telomeres and mediates DNA repair by encasing DNA ends. Nat. Struct. Mol. Biol. *24*, 588–595.

Müller, C.A., Hawkins, M., Retkute, R., Malla, S., Wilson, R., Blythe, M.J., Nakato, R., Komata, M., Shirahige, K., de Moura, A.P., and Nieduszynski, C.A. (2014). The dynamics of genome replication using deep sequencing. Nucleic Acids Res. *42*, e3.

Park, S., Patterson, E.E., Cobb, J., Audhya, A., Gartenberg, M.R., and Fox, C.A. (2011). Palmitoylation controls the dynamics of budding-yeast heterochromatin via the telomere-binding protein Rif1. Proc. Natl. Acad. Sci. USA *108*, 14572–14577.

Peace, J.M., Ter-Zakarian, A., and Aparicio, O.M. (2014). Rif1 regulates initiation timing of late replication origins throughout the S. cerevisiae genome. PLoS ONE *9*, e98501.

Rhind, N., and Gilbert, D.M. (2013). DNA replication timing. Cold Spring Harb. Perspect. Med. *3*, 1–26.

Schmid, M., Durussel, T., and Laemmli, U.K. (2004). ChIC and ChEC: Genomic mapping of chromatin proteins. Mol. Cell *16*, 147–157.

Shi, T., Bunker, R.D., Mattarocci, S., Ribeyre, C., Faty, M., Gut, H., Scrima, A., Rass, U., Rubin, S.M., Shore, D., and Thomä, N.H. (2013). Rif1 and Rif2 shape telomere function and architecture through multivalent Rap1 interactions. Cell *153*, 1340–1353.

Shyian, M., Mattarocci, S., Albert, B., Hafner, L., Lezaja, A., Costanzo, M., Boone, C., and Shore, D. (2016). Budding yeast Rif1 controls genome integrity by inhibiting rDNA replication. PLoS Genet. *12*, e1006414.

Siddiqui, K., On, K.F., and Diffley, J.F. (2013). Regulating DNA replication in eukarya. Cold Spring Harb. Perspect. Biol. Published online September 1, 2013. https://doi.org/10.1101/cshperspect.a012930.

Siow, C.C., Nieduszynska, S.R., Müller, C.A., and Nieduszynski, C.A. (2012). OriDB, the DNA replication origin database updated and extended. Nucleic Acids Res. *40*, D682–D686.

Soriano, I., Morafraile, E.C., Vázquez, E., Antequera, F., and Segurado, M. (2014). Different nucleosomal architectures at early and late replicating origins in Saccharomyces cerevisiae. BMC Genomics *15*, 791.

Sreesankar, E., Senthilkumar, R., Bharathi, V., Mishra, R.K., and Mishra, K. (2012). Functional diversification of yeast telomere associated protein, Rif1, in higher eukaryotes. BMC Genomics *13*, 255.

Zentner, G.E., Kasinathan, S., Xin, B., Rohs, R., and Henikoff, S. (2015). ChEC-seq kinetics discriminates transcription factor binding sites by DNA sequence and shape in vivo. Nat. Commun. *6*, 8733.